specifically biotinylated macromolecules on a lipid layer, facilitating their crystallization in two dimensions.

REFERENCES

Albrecht, O. (1983) *Thin Solid Films 99*, 227-232.
Bayer, E. A., & Wilchek, M. (1974) *Methods Enzymol. 34*, 265-267.
Bayer, E. A., Rivnay, B., & Skutelsky, E. (1979) *Biochim. Biophys. Acta 550*, 464-473.
Cuatrecasas, P., & Wilchek, M. (1968) *Biochem. Biophys. Res. Commun. 33*, 235-239.
Dorn, K. (1981) PhD-Dissertation, Mainz Universität.
Garlick, R. K., & Giese, R. W. (1988) *J. Biol. Chem. 263*, 210-215.
Green, N. M. (1963) *Biochem. J. 89*, 599-604.
Green, N. M. (1975) *Adv. Protein Chem. 29*, 85-133.
Hashimoto, K., Loader, J. E., & Kinsky, S. C. (1986) *Biochim. Biophys. Acta 856*, 556-565.
Hiller, Y., Gershoni, J. M., Bayer, E. A., & Wilchek, M. (1987) *Biochem. J. 248*, 167-171.
Hofmann, K., Wood, S. W., Brinton, C. C., Montilbeller, J. A., & Finn, F. M. (1980) *Proc. Natl. Acad. Sci. U.S.A. 77*, 4666-4668.
Laschewski, A., Ringsdorf, H., Schmidt, G., & Schneider, J. (1987) *J. Am. Chem. Soc. 109*, 788-796.
Lösche, M., & Möhwald, H. (1984) *Rev. Sci. Instrum. 55*, 1968-1972.
Loughrey, H., Bally, M. B., & Cullis, P. R. (1987) *Biochim. Biophys. Acta 901*, 157-160.
McConnell, H. M., Tamm, L. K., & Weis, R. W. (1984) *Proc. Natl. Acad. Sci. U.S.A. 81*, 3249-3253.
Meller, P. (1988) *Rev. Sci. Instrum. 59*, 2225-2231.
Nargessi, R. D., & Smith, D. S. (1986) *Methods Enzymol. 122*, 67-72.
Neumann, R., & Ringsdorf, H. (1986) *J. Am. Chem. Soc. 108*, 487-490.
Reed, R. A., Mattai, J., & Shipley, G. G. (1987) *Biochemistry 26*, 824-832.
Ribi, H. O., Reichard, P., & Kornberg, R. D. (1987) *Biochemistry 26*, 7974-7979.
Ribi, H. O., Ludwig, D. S., Lynne Mercer, K., Schoolnik, G. K., & Kornberg, R. D. (1988) *Science 239*, 1272-1276.
Roffman, E., Meromsky, L., Ben-Hur, H., Bayer, E. A., & Wilchek, M. (1986) *Biochem. Biophys. Res. Commun. 136*, 80-85.
Uzgiris, E. E. (1987) *Biochem. J. 242*, 293-296.
Uzgiris, E. E., & Kornberg, R. D. (1983) *Nature 301*, 125-129.
Wilchek, M., & Bayer, E. A. (1988) *Anal. Biochem. 171*, 1-32.

Kinetics of the Purified Glucose Transporter. Direct Measurement of the Rates of Interconversion of Transporter Conformers†

James R. Appleman*,‡ and Gustav E. Lienhard§

Department of Biochemical and Clinical Pharmacology, St. Jude Children's Research Hospital, Memphis, Tennessee 38101, and Department of Biochemistry, Dartmouth Medical School, Hanover, New Hampshire 03756

Received April 5, 1989; Revised Manuscript Received June 1, 1989

ABSTRACT: There is considerable evidence that the mechanism of glucose transport by the transporter of human erythrocytes is one in which the transporter oscillates between two conformations, T_o and T_i. Each conformer possesses a single glucose binding site that in vivo faces either the extracellular space (conformer T_o) or the cytoplasm (conformer T_i). In this study, the interconversions of these conformers in the absence and presence of D-glucose have been directly observed by means of the stopped-flow method with fluorescence detection. Nearly unidirectional conversion of one conformer to the other was accomplished by rapidly mixing purified transporter (a mixture of T_o and T_i) with either 4,6-ethylidene-D-glucose, which preferentially binds to T_o, or phenyl β-D-glucoside, which preferentially binds to T_i. The values of the individual rate constants for the conversion of T_i to T_o and vice versa in the absence and presence of D-glucose at 10.0 °C have been obtained, and these show that the kinetics are consistent with the alternating conformation model for transport. Conformational change occurs much more rapidly with glucose bound to the transporter. Furthermore, the activation energy E_a for conformer interconversion is much less when glucose is bound than for unliganded transporter. For example, E_a is approximately 28 kcal/mol for $T_i \rightarrow T_o$ versus 17 kcal/mol for $T_i + S \rightarrow T_oS$, where S is glucose. The α-anomer of glucose was 37% more effective than the β-anomer in speeding the interconversion. Analysis of the fluorescence change upon mixing the transporter with several concentrations of 4,6-ethylidene-D-glucose revealed that the intrinsic fluorescence of the T_o form is less than that of the T_i form by 20% or more.

The glucose transporter of human erythrocytes is a transport system of the facilitated diffusion type that can be purified in abundance (Baldwin et al., 1982). The amino acid sequence of the transporter indicates that the polypeptide chain weaves across the membrane 12 times (Mueckler et al., 1985). The mechanism of transport is most probably one in which the transporter oscillates between two conformations. One conformer, T_o, exhibits an extracellular glucose binding site. The other conformer, T_i, exhibits an inward-facing glucose binding

† This work was supported by Research Grant GM 22996 (to G.E.L.) from the National Institutes of Health.

‡ St. Jude Children's Research Hospital.
§ Dartmouth Medical School.

0006-2960/89/0428-8221$01.50/0

Scheme I

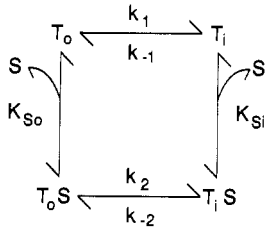

site. When the substrate binding site is occupied (T_oS or T_iS species), the conformational change results in the translocation of the bound glucose across the membrane. Since the transporter is fixed in the plane of the lipid bilayer, translocation occurs by passage of the glucose through the protein rather than through rotation of the protein–glucose complex across the plane of the bilayer. There is strong evidence in support of this mechanism [reviewed by Baldwin and Lienhard (1981) and Walmsley (1988)], although some findings may remain to be reconciled with it (Naftalin, 1988; Carruthers, 1988).

The kinetic scheme corresponding to this mechanism is shown in Scheme I, in which the K's are dissociation constants and the k's are rate constants. We have previously obtained evidence in support of this scheme by spectroscopically detecting and measuring the rate of the T_i to T_o conversion (Appleman & Lienhard, 1985). This was accomplished by monitoring the protein fluorescence as a function of time when the purified glucose transporter, reconstituted in unsealed membranes, was mixed with 4,6-ethylidene-D-glucose (EGlc)[1] in a stopped-flow apparatus. EGlc is a nontransported glucose derivative that binds preferentially to the T_o conformer. Mixing EGlc with the transporter produces a rapid, first-order decrease in intrinsic protein fluorescence. According to several criteria (Appleman & Lienhard, 1985), this first-order transient is due to the conversion of T_i to T_o, which is immediately trapped by complexation with EGlc. The fact that the intrinsic fluorescence of T_oEGlc is less than that of T_i allows detection of this single half-turnover event.

In the present study, we have expanded this approach for determination of the pre-steady-state kinetics of the transporter. Performance of the measurements at 10 °C, rather than at 25 °C, has allowed determination of rates at lower concentrations of EGlc than were used in our initial study. Moreover, the rates of conformational change in the opposite direction (T_o to T_i) have been measured through the use of phenyl β-D-glucoside (PhGlc), a derivative that binds preferentially to the T_i conformer (Barnett et al., 1975). As a consequence, it has been possible to determine the values of the four rate constants required for a complete kinetic description of transport according to Scheme I (k_1, k_{-1}, k_2/K_{So}, k_{-2}/K_{Si}). In addition, we have determined the relative fluorescence intensities of T_o and T_i, the effect of glucose anomer on the rate constant for the combination of glucose binding and conformational change (k_{-2}/K_{Si}), and the effect of temperature on rate constants involving the conformational changes of T_i and T_iS.

Experimental Procedures

Materials. EGlc was purchased from Pfalz and Bauer, Inc., and purified by chromatography on cellulose and treatment with activated charcoal (Gorga & Lienhard, 1981). PhGlc and α-D-glucose were purchased from Sigma. β-D-Glucose was purchased from Pfanstiehl.

Scheme II

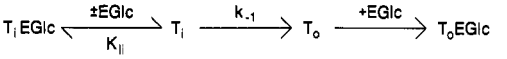

Scheme III

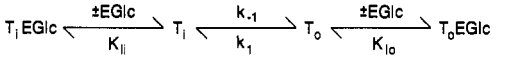

The glucose transporter was purified and characterized as described previously (Baldwin et al., 1982; Appleman & Lienhard, 1985). This preparation consists of transporter reconstituted into membranes of erythrocyte lipids that accompany it during purification; typically, the concentrations of protein and lipid are about 150 and 500 μg/mL, respectively. Both cytosolic and extracellular domains are accessible to ligands as demonstrated by the ability of trypsin to cleave the transporter and neuraminidase to release sialic acid residues in the absence of detergent (Appleman & Lienhard, 1985).

Kinetic Measurements. Kinetic measurements were performed with a Dionex D-110 stopped-flow spectrophotometric system, as described previously (Appleman & Lienhard, 1985). In the presence of PhGlc, the wavelength of light used to excite protein fluorescence was increased from 280 nm to as high as 295 nm to reduce inner filter effects caused by absorbance by PhGlc. For all experiments the final concentration of transporter was 7.5 μg/mL; the buffer was 100 mM NaCl, 1 mM EDTA, and 50 mM Tris-HCl, pH 7.2, at 10 °C. The temperature was 10.0 °C except where noted.

Calculation of Rate Constants. When the transporter was mixed with EGlc or PhGlc, the intrinsic fluorescence of the protein was altered in a time-dependent process. The fluorescence intensities at each time were corrected for photolysis, and the best-fit value of the first-order rate constant (k_{obs}) governing this change in protein fluorescence was calculated according to the methods that we have described previously (Appleman & Lienhard, 1985).

Results and Discussion

Determination of the Values of k_1 and k_{-1}. Previously we have reported that a fluorescence transient is observed when the glucose transporter is mixed with EGlc in a stopped-flow apparatus (Appleman & Lienhard, 1985). The time course of quenching of protein fluorescence is a first-order process (rate constant, k_{obs}). The value of the rate constant k_{-1} controlling the rate of conversion of T_i to T_o was calculated from the dependence of k_{obs} on EGlc concentration. At saturating EGlc concentrations, the process corresponding to EGlc binding is shown in Scheme II, in which K_{Ii} is the dissociation constant for EGlc binding to T_i. Immediately after mixing, the fraction of transporter preexisting as the T_i form rapidly equilibrates with EGlc, and the resulting T_iEGlc complex cannot directly undergo the conversion to the T_o conformer. At equilibrium, about 90% of the transporter is in the T_oEGlc form because EGlc affinity is much higher for T_o than for T_i (Baker et al., 1978; Deves & Krupa, 1978). Thus, at saturating concentrations of EGlc, k_{obs} equals $k_{-1}/(1 + [EGlc]/K_{Ii})$. At low (subsaturating) concentrations of EGlc, the amplitude of the fluorescence decay becomes smaller. This fact, coupled with the very fast reaction rates, prevented the accurate measurement of k_{obs} at low EGlc concentrations at 25 °C in our previous studies.

By reducing the temperature to 10 °C, it became possible to measure k_{obs} accurately at subsaturating concentrations of EGlc. The reaction path under these conditions is shown in

[1] Abbreviations: EGlc, 4,6-ethylidene-D-glucose; PhGlc, phenyl β-D-glucoside.

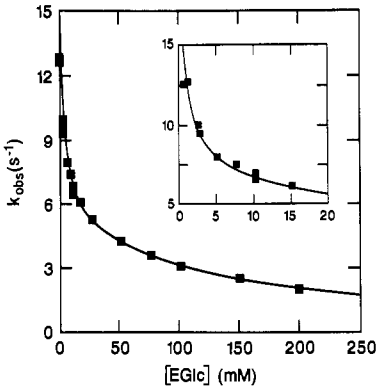

FIGURE 1: Dependence of k_{obs} upon EGlc concentration. The value of the rate constant k_{obs} at each concentration of EGlc was calculated as described under Experimental Procedures from the time course of fluorescence decrease that occurs when glucose transporter is mixed with EGlc. The inset shows the values at low EGlc on an expanded abscissa. Each value for k_{obs} is the average of at least five determinations, for which the standard deviation was less than 5% of the average value. The smooth curve through the points was generated by the use of eq 1 and the best values of k_1, k_{-1}, K_{Io}, and K_{Ii} (see text).

Scheme III, in which K_{Io} is the dissociation constant for EGlc with respect to the T_o conformer. With the assumption that the interconversion of T_o and T_i is slow compared to EGlc binding steps, these binding steps may be treated as being at equilibrium at all but the earliest times. When transporter is mixed with EGlc, transporter in the T_i form rapidly equilibrates with T_iEGlc. Similarly, T_o rapidly equilibrates with T_oEGlc. These equilibrations are too fast to monitor by the technique employed in this study. A slower phase follows as all transporter species come to the new equilibrium dictated by the concentration of EGlc. This second phase is a first-order process described by the rate constant k_{obs}. The dependence of k_{obs} on the concentration of EGlc is given by

$$k_{obs} = \frac{k_1}{1 + [EGlc]/K_{Io}} + \frac{k_{-1}}{1 + [EGlc]/K_{Ii}} \quad (1)$$

At low EGlc concentrations the final equilibrium is not substantially different from that achieved immediately after mixing, and the rate at which this final equilibrium is reached is rapid. At higher EGlc concentrations (where most of the transporter is in the liganded forms immediately upon mixing), this rate becomes substantially slower. The fluorescence transient observed when transporter is mixed with EGlc reflects the changes in concentration of the various transporter species as the system goes to equilibrium. The first-order rate constant governing this transient, k_{obs}, is the same as that given by eq 1, since it can be shown that the value of this constant is independent of the fluorescence intensities of the various transporter species (T_iEGlc, T_i, T_o, T_oEGlc).

The dependence of k_{obs} on the concentration of EGlc was determined over a wide range of EGlc concentrations (Figure 1). When the data were fitted to eq 1, the following values[2] for the constants were obtained: k_1, 9.5 ± 0.6 s^{-1}; k_{-1}, 5.2 ± 0.7 s^{-1}; K_{Io}, 2.5 ± 0.7 mM; and K_{Ii}, 116.8 ± 33.3 mM. The correct assignment of constants to the values in eq 1 (for example, k_1 not k_{-1}, is equal to 9.5 s^{-1}) followed from the fact that EGlc has a much higher affinity for T_o than for T_i.

[2] The values of these constants giving the best fit in a least-squares sense of the data (i.e., k_{obs}) to this equation were calculated by using the NLLSQ computer program that employs Marguardt's strategy for the solution of nonlinear least-squares problems (Christian & Tucker, 1972). This method of data analysis was used in determination of all kinetic and binding constants reported herein.

Scheme IV

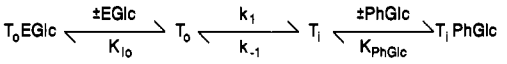

Since the ratio k_{-1}/k_1 is equal to the equilibrium constant for the distribution of the transporter between the T_o and T_i forms, the ratio of T_i to T_o at 10 °C is 65:35. The value of the overall dissociation constant for EGlc binding, K_I, may be calculated from the above values since

$$K_I = \frac{(k_1 + k_{-1})K_{Io}K_{Ii}}{k_1K_{Io} + k_{-1}K_{Ii}}$$

The value of K_I calculated from this equation is equal to 6.7 mM, in good agreement with the value of 5.2 mM obtained by equilibrium titration with fluorescence detection at 10 °C [data not shown; see Gorga and Lienhard (1982) for the method].

A more direct determination of k_1 could in principle be made from experiments in which transporter is mixed with a sugar that binds preferentially to the T_i conformer. We have attempted such measurements with the sugar phenyl glucoside (PhGlc), which complexes at least 90% of the transporter in the T_i form at equilibrium (Barnett et al., 1975). After mixing transporter with PhGlc, we consistently observed a very small increase in fluorescence at early times. However, accurate determination of k_{obs} was impractical because the amplitude of the transient is of nearly the same magnitude as instrumental noise. Additional complications included absorbance by PhGlc at 280 nm and a time-dependent decrease in fluorescence. This decrease was also observed in solutions in which transporter was preincubated with PhGlc and in solutions containing PhGlc alone. The rate of the fluorescence decrease was dependent upon the concentration of PhGlc and required exposure to light; thus, it is presumably due to a photochemical reaction of PhGlc. These experimental difficulties were exacerbated by the fact that only 35% of the transporter exists as T_o prior to mixing with PhGlc (see above).

Since the net reaction under observation is the conversion of T_o to T_iPhGlc, it seemed possible that the amplitude of the fluorescence transient could be increased by increasing the initial concentration of transporter in a T_o form. This was accomplished by preincubating the transporter with 5 mM EGlc and then mixing this solution with an equal volume of a PhGlc solution in the stopped-flow apparatus. In the presence of 5 mM EGlc, T_oEGlc and T_o constitute 62% of the total transporter prior to mixing with PhGlc. Thus, with these conditions, the reaction under observation consists of the conversion of both T_oEGlc and T_o to T_iPhGlc. Since the final concentration of EGlc is small compared to K_{Ii}, the reaction scheme for these experimental conditions is that shown in Scheme IV, in which K_{PhGlc} is the dissociation constant for PhGlc with respect to the T_i conformer. The equation defining k_{obs} for this scheme is

$$k_{obs} = \frac{k_1}{1 + [EGlc]/K_{Io}} + \frac{k_{-1}}{1 + [PhGlc]/K_{PhGlc}} \quad (2)$$

This experimental approach yielded time-dependent increases in protein fluorescence of a magnitude that allowed accurate evaluation of k_{obs}. The values of k_{obs} for the fluorescence transients when transporter preincubated with 5 mM EGlc was mixed with several intermediate concentrations of PhGlc are presented in Table I. Experimental details are reported in the accompanying legend.[3] The average value

Table I: k_{obs} at Varying Concentrations of PhGlc[a]

[PhGlc] (mM)	k_{obs} (s^{-1})	k_1 (s^{-1})
1.25	6.8	9.2
2.50	5.3	7.8
5.00	4.9	8.3

[a] Transporter preincubated with 5 mM EGlc was mixed with an equal volume of PhGlc, and k_{obs} was determined from the time course of fluorescence increase. Tabulated values for PhGlc concentration are for the final reaction mixture. Each value of k_{obs} is the average of at least five determinations, for which the standard deviation was less than 5%. The values of k_1 were calculated from those of k_{obs} by means of eq 2 in the text, with the values of K_{Io} and k_{-1} fixed at 2.5 mM and 5.2 s^{-1} (see text) and K_{PhGlc} set at 0.9 mM, respectively. The latter value was determined from the concentration dependence of the inhibition by PhGlc of the rate of cytochalasin B binding to the T_i conformer (data not shown).[3] This value agrees with a value of 1.2 mM for the overall dissociation constant for PhGlc, as measured by inhibition of the equilibrium binding of [^{3}H]cytochalasin B at 20 °C [data not shown; method of Gorga and Lienhard (1981)].

of 8.4 ± 0.7 s^{-1} for k_1 obtained by this alternate method is in good agreement with the value of 9.5 ± 0.6 s^{-1} from the experiments involving transporter mixed with EGlc alone (Figure 1).

Relative Fluorescent Intensities of T_i, T_o, T_iEGlc, and T_oEGlc. F^0, the fluorescence intensity attributable to transporter species immediately after transporter was mixed with EGlc, can be expressed as

$$F^0 = f_{TiEGlc}[T_iEGlc]^0 + f_{Ti}[T_i]^0 + f_{To}[T_o]^0 + f_{ToEGlc}[T_oEGlc]^0$$

where $[T_iEGlc]^0$, $[T_i]^0$, $[T_o]^0$, and $[T_oEGlc]^0$ are the concentrations of the various transporter species before significant interconversion of T_o and T_i occurs and f_{TiEGlc}, f_{Ti}, f_{To}, and f_{ToEGlc} are constants such that the fluorescence intensity attributable to each species is equal to the concentration of the species multiplied by the corresponding constant (for example, $F^0_{To} = f_{To}[T_o]^0$). With the assumption that binding of EGlc to T_o and T_i is at equilibrium it follows that

$$F^0 = \left[\left(\frac{f_{TiEGlc}[EGlc] + f_{Ti}K_{Ii}}{[EGlc] + K_{Ii}}\right)\left[\frac{1}{1 + K_1}\right] + \left(\frac{f_{ToEGlc}[EGlc] + f_{To}K_{Io}}{[EGlc] + K_{Io}}\right)\left[\frac{K_1}{1 + K_1}\right]\right][T]_{tot} \quad (3a)$$

where $[T]_{tot}$ is the sum of the concentration of all transporter species, $K_1 = k_{-1}/k_1$, and K_{Ii} and K_{Io} have been defined previously. At equilibrium, the fluorescence intensity due to transporter species is

$$F^{equ} = f_{TiEGlc}[T_iEGlc]^{equ} + f_{Ti}[T_i]^{equ} + f_{To}[T_o]^{equ} + f_{ToEGlc}[T_oEGlc]^{equ}$$

where $[T_iEGlc]^{equ}$, $[T_i]^{equ}$, $[T_o]^{equ}$, and $[T_oEGlc]^{equ}$ are the concentrations of the transporter species at equilibrium. From the equilibria relating the concentrations of these species, it can be seen that

$$F^{equ} = \left(\frac{f_{TiEGlc}[EGlc]/K_{Ii} + f_{Ti} + (f_{To} + f_{ToEGlc}[EGlc]/K_{Io})K_1}{[EGlc]/K_{Ii} + 1 + (1 + [EGlc]/K_{Io})K_1}\right) \times [T]_{tot} \quad (3b)$$

The percent of fluorescence quenching, Q, associated with the redistribution of transporter species is defined by

$$Q = (1 - F^{equ}/F^0) \times 100\%$$

In the ratio of F^{equ} to F^0, the f's can be replaced by relative fluorescence constants, f^*'s, where $f^*_{TiEGlc} = f_{TiEGlc}/f_{Ti}$, $f^*_{To} = f_{To}/f_{Ti}$, and $f^*_{ToEGlc} = f_{ToEGlc}/f_{Ti}$. By definition $f^*_{Ti} = 1$. In this fashion the relative fluorescence properties of the transporter species T_o, T_oEGlc, T_iEGlc, and T_i may be calculated from the dependence of Q on the concentration of EGlc and the known values of k_1, k_{-1}, K_{Io}, and K_{Ii} (see above). In reality, the measured values of F^{equ} and F^0 include some contribution, F_{nonsp}, due to sources such as light scattering or nontransporter contaminants, and thus the measured value of the initial fluorescence intensity, $F^{0\prime}$, equals $F^0 + F^{nonsp}$. Similarly, the measured value of the final fluorescence intensity, $F^{equ\prime}$, equals $F^{equ} + F_{nonsp}$. The observed quenching coefficient, Q', equals $(1 - F^{equ\prime}/F^{0\prime}) \times 100\%$. If a new constant, r, is defined such that $r = F_{nonsp}/F^{0\prime}$, it may be shown that

$$Q' = [(1 - r) + (r - 1)F^{equ}/F^0] \times 100\% \quad (4)$$

For various assumed values of r, values for f^*_{TiEGlc}, f^*_{To}, and f^*_{ToEGlc} were calculated by fitting the experimentally measured

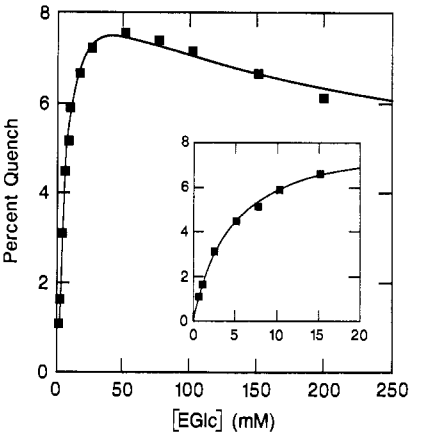

FIGURE 2: Dependence of the percent of fluorescence quench Q' upon EGlc concentration. The inset shows the values at low EGlc on an expanded abscissa. Each value for the percent quench is the average of at least five determinations, for which the standard deviation was less than 5% of the average value. The smooth curve through the points was calculated from the combination of eq 3a, 3b, and 4 describing Q', from the best values of k_1, k_{-1}, K_{Io}, and K_{Ii} in the text, and from the values of f^*_{To}, f^*_{ToEGlc}, and f^*_{TiEGlc} corresponding to $r = 0$ in Table II.

Table II: Relative Fluorescence Intensities of the Conformers of Transporter and Transporter–EGlc[a]

r ($F_{nonsp}/F^{0\prime}$)	f_{ToEGlc}/f_{Ti}	f_{To}/f_{Ti}	f_{TiEGlc}/f_{Ti}
0.0	0.85	0.81	0.91
0.2	0.81	0.77	0.89
0.4	0.75	0.70	0.85
0.6	0.65	0.57	0.77

[a] The best-fit values for f_{ToEGlc}/f_{Ti} (f^*_{ToEGlc}), f_{To}/f_{Ti} (f^*_{To}), and f_{TiEGlc}/f_{Ti} (f^*_{TiEGlc}) were obtained by fitting the data in Figure 2 to eq 4 at several assumed values for the proportion of nonspecific fluorescence (r).

[3] When low concentrations of cytochalasin B are mixed with transporter, the time course of binding of this ligand to the T_i conformer can be directly monitored by fluorescence quenching (data not shown). The initial rate of binding increases linearly with cytochalasin B concentration. At any concentration of cytochalasin B, this rate is decreased by the presence of PhGlc. The value of K_{PhGlc} was calculated from the dependence of the observed first-order rate constant governing the time course of CB binding to the T_i conformer, k_{obs}, on PhGlc concentration. It may be shown that $k_{obs} = k_{CB}[\text{cytochalasin B}]/(1 + [PhGlc]/K_{PhGlc})$, where k_{CB} is the second-order rate constant in the absence of PhGlc.

Scheme V

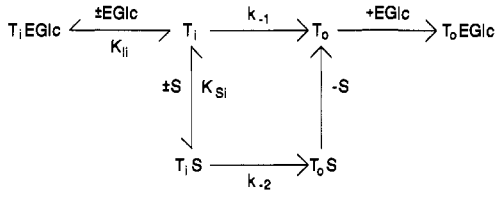

Scheme VI

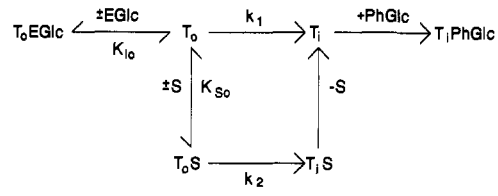

dependence of Q' on the concentration of EGlc to eq 4, where the ratio F^{equ}/F^0 is defined by the ratio of eq 3b to 3a. Values for f^*'s obtained in this way at several different assumed values for r are given in Table II. Figure 2 shows the experimentally measured dependence of Q' on EGlc concentration; the smooth curve through the points has been calculated from parameter values in Table II corresponding to r equals zero (no nonspecific contribution). The quality of the fit is quite good.

The relative fluorescence intensities of the species T_i, T_iEGlc, T_o, and T_oEGlc are 1.0, 0.89, 0.77, and 0.81, at an r of 0.2 (Table II). The values are similar at other r values in the range expected for the fraction of nonprotein fluorescence (0–0.4). Thus, the immediate cause of the fluorescence quench that is observed when the transporter is mixed with EGlc is not the binding of EGlc to T_o, which by itself would lead to a small fluorescence increase, but the conversion of T_i to T_o, which is only about 80% as fluorescent as T_i.

Determination of the Values for k_{-2}/K_{Si} and k_2/K_{So}. The ratio k_{-2}/K_{Si} is the second-order rate constant for the reaction $T_i + S \rightarrow T_oS$ when glucose concentrations are small compared to K_{Si}. The ratio k_2/K_{So} is the equivalent constant for the reaction $T_o + S \rightarrow T_iS$. We have previously demonstrated how k_{-2}/K_{Si} may be determined from the linear dependence of k_{obs} on glucose concentration when transporter is mixed with a fixed saturating concentration of EGlc (Appleman & Lienhard, 1985). The addition of low concentrations of glucose enhances the rate of the fluorescence transients observed under such conditions. For sufficiently high EGlc concentrations, almost all of the transporter is trapped in the T_oEGlc form at equilibrium. Scheme V describes the pathways for conformational change in the presence of glucose. In Scheme V K_{Si} is the dissociation constant for glucose binding to T_i and k_{-2} is the rate constant for the conversion of T_iS to T_oS. For glucose concentrations low compared to K_{Si}

$$k_{obs} = \frac{k_{-1} + k_{-2}[S]/K_{Si}}{1 + [EGlc]/K_{Ii}}$$

and k_{obs} increases linearly with increasing glucose concentration. Now consider a case in which transporter preincubated with EGlc is simultaneously mixed with a low concentration of glucose and a saturating concentration of PhGlc. The pathways for conformational change then become those shown in Scheme VI. For such a reaction scheme

$$k_{obs} = \frac{k_1 + k_2[S]/K_{So}}{1 + [EGlc]/K_{Io}}$$

In reality both Schemes V and VI oversimplify the true situation. In Scheme V the fact that EGlc binding to T_o is an equilibrium process, not an irreversible step, is ignored. Scheme VI disregards the same fact for PhGlc binding to T_i; also neglected is the weak binding of EGlc to T_i. The single equation describing k_{obs} for the complete scheme (combination of Schemes V and VI) at glucose concentrations that are small with respect to K_{So} and K_{Si} is

$$k_{obs} = \frac{k_{-1} + k_{-2}[S]/K_{Si}}{1 + [EGlc]/K_{Ii} + [PhGlc]/K_{PhGlc}} + \frac{k_1 + k_2[S]/K_{So}}{1 + [EGlc]/K_{Io}} \quad (5)$$

When transporter is mixed with EGlc and glucose, the first term of eq 5 predominates and protein quenching is observed (net conversion of T_i to T_o). When transporter preincubated with EGlc is mixed with PhGlc and glucose, the second term predominates and an increase in protein fluorescence is observed (net conversion of T_o to T_i). The dependence of k_{obs} on glucose concentration for both kinds of experiments is shown in Figure 3. All of the data in this figure were simultaneously fitted to eq 5 with the values of k_1, k_{-1}, K_{Io}, K_{Ii}, and K_{PhGlc} fixed at 9.5 s^{-1}, 5.2 s^{-1}, 2.5 mM, 116.8 mM (see above), and 0.9 mM (see legend to Table I), respectively. The best-fit values from this analysis for k_2/K_{So} and k_{-2}/K_{Si} are 65.6 ± 1.6 and 30.7 ± 1.0 mM^{-1} s^{-1}, respectively. Each straight line through the experimentally determined values of k_{obs} has been calculated from these parameters for the particular condition of constant [EGlc] and [PhGlc] (where present). The excellent fit to these data supports the assumption that the concentration of glucose is small compared to both K_{Si} and K_{So} over the range of glucose concentration used here. Attempts to measure k_{obs} at high concentrations of glucose, from which the individual values of k_{-2}, K_{Si}, k_2, and K_{So} could be calculated by fitting k_{obs} as a function of glucose concentration (equations not shown), were unsuccessful because reaction rates were so high as to be unmeasurable by the stopped-flow technique.

Evaluation of Scheme I from the Measured Values of k_1, k_{-1}, k_2/K_{So}, and k_{-2}/K_{Si}. There are two pathways by which T_o and T_oS may interconvert in Scheme I. The first pathway is shown in Scheme VII, andthe second pathway is shown in Scheme VIII. It follows that

$$[S]/K_{So} = (k_1/k_{-1})(k_{-2}/k_2)[S]/K_{Si}$$

and so $k_{-2}/K_{Si} = (k_{-1}/k_1)(k_2/K_{So})$. From the values of the individual constants, k_{-2}/K_{Si} equals 30.7 mM^{-1} s^{-1}, while $(k_{-1}/k_1)(k_2/K_{So})$ equals 35.8 mM^{-1} s^{-1}. This good agreement provides evidence that Scheme I is a valid kinetic model for the mechanism of glucose transport via facilitated diffusion.

Scheme VII

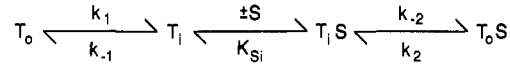

Scheme VIII

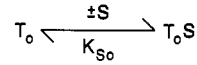

Comparison of k_{-2}/K_{Si} for the Anomers of D-Glucose. After a period in solution, D-glucose consists of a 37:63 mixture of the α- and β-anomers, respectively (Angyal, 1968). Since the kinetics of transport of each anomer may be different, we determined the value of k_{-2}/K_{Si} for each anomer in a manner similar to that used in measuring this parameter for the equilibrium mixture (see Figure 3).

Crystalline α- or β-D-glucose was dissolved in buffer containing EGlc at 10 °C and subsequently mixed with the transporter in the stopped-flow apparatus. The total elapsed

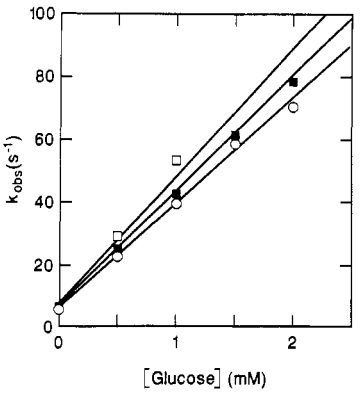

FIGURE 3: Dependence of k_{obs} on glucose concentration. (○) Transporter was simultaneously mixed with EGlc and glucose such that the final concentration of EGlc was 20 mM. The reaction was monitored by the decrease in protein fluorescence as the T_oEGlc complex was formed. (□, ■) Transporter preincubated with 5 mM EGlc was simultaneously mixed with PhGlc and glucose. The reaction was monitored by the increase in protein fluorescence as the T_iPhGlc complex was formed. Final EGlc concentration was 2.5 mM. Final PhGlc concentrations were 2.5 (□) and 5.0 (■) mM. Each value for k_{obs} is the average of at least five determinations, for which the standard deviation was less than 7.5% of the average value. Each straight line was generated from eq 5 with values for the constants given in the text.

Table III: Values of k_{-2}/K_{Si} for the Glucose Anomers[a]

species	[glucose] (mM)	[EGlc] (mM)	k_{obs} (s^{-1})	k_{-2}/K_{Si} (s^{-1} mM^{-1})
α-D-glucose	1.00	19.6	49.1	52.3
β-D-glucose	1.00	19.6	36.6	37.7
equilibrium mixture				
obsd	1.00	20.0	38.6	40.0
theor	1.00	20.0	41.2	

[a] Transporter was mixed with EGlc and glucose and the time course of fluorescence quenching monitored. Each value of k_{obs} is the average of six determinations, the standard deviation for which was less than 3%. The value of k_{-2}/K_{Si} was calculated from $k_{-2}/K_{Si} = k_{obs}(1 + [EGlc]/K_{Ii}) - k_{-1}$ (eq 5, with the small contribution from the second term neglected), where K_{Ii} and k_{-1} equal 116.8 mM and 5.2 s^{-1}, respectively. The theoretical value of k_{obs} for the equilibrium mixture was calculated from $k_{obs,theor} = (k_{-1} + (k_{-2}/K_{Si})_\alpha[S]_\alpha + (k_{-2}/K_{Si})_\beta[S]_\beta/(1 + [EGlc]/K_{Ii}). + [EGlc]/K_{Ii})$.

time between addition of glucose to the buffered EGlc solution and completion of the experimental measurements was 5 min; from the rate constant for mutarotation under similar conditions [5.5×10^{-3} min^{-1} at 10 °C, by interpolation (Carruthers & Melchior, 1985)], less than 3% of each anomer underwent mutarotation in this period. Table III presents the results. The value of k_{-2}/K_{Si} for the α-anomer is 37% larger than that for the β-anomer. Also note that there is good agreement between the experimentally determined and calculated values of k_{obs} for the equilibrium mixture of anomers.

The values of k_{-2}/K_{Si} and k_2/K_{So} reported in the previous section are weighted averages of the corresponding ratios for the concentration of the α- and β-anomers. For example

$$(k_{-2}/K_{Si})_{obs} = \frac{(k_{-2}/K_{Si})_\alpha[S]_\alpha + (k_{-2}/K_{Si})_\beta[S]_\beta}{[S]_\alpha + [S]_\beta}$$

where S_α and S_β make up 37% and 63% of the total glucose, respectively. The fact that k_{-2}/K_{Si} and k_2/K_{So} are weighted averages does not invalidate the internal consistency of the values of rate and binding constants with respect to the kinetic model for transport in Scheme I presented in the previous section.

Prior to this study Carruthers and Melchior (1985) reported that the rates of uptake of 100 mM α- and β-D-glucose into

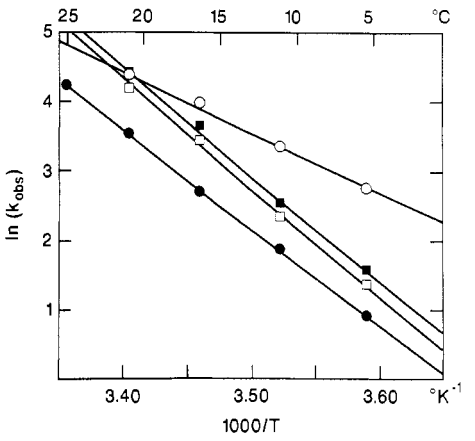

FIGURE 4: Temperature dependence of k_{obs} with varying EGlc and glucose concentrations. Each value of k_{obs} is the average of at least five determinations, the standard deviation for which was less than 7.5% of the average. The values for k_{obs} at 10.0 °C in Figure 1 are about 30% lower than those in this set of experiments measured under the same conditions at 10.7 °C; the explanation may be these measurements were made with a different preparation of transporter than was used for all the other kinetics measurements in this study. The activation energy, E_a, was calculated by linear regression.

condition	symbol	[EGlc] (mM)	[glucose] (mM)	E_a (kcal/mol)	definition of k_{obs}
A	■	5	0	30.8	eq 1
B	□	10	0	31.4	eq 1
C	●	50	0	28.2	$k_{-1}/(1 + [EGlc]/K_{Ii})$
D	○	50	1	17.4	$k_{-2}[S]/\{K_{Si}(1 + [EGlc]/K_{Ii})\}$

human erythrocytes at 0.7 and 37 °C are the same. However, the magnitudes of the standard deviation in their data (from 25% to 90% of the value for the half-time) were such that a small difference would not have been detected.

Temperature Dependence of k_{obs}. The Arrhenius diagram of Figure 4 shows that the logarithm of k_{obs} is a linear function of the reciprocal of the absolute temperature under four different experimental conditions (see legend accompanying Figure 4). Because k_{obs} is a complex combination of rate and dissociation constants, the activation energy, E_a, calculated at each condition is not in a strict sense the activation energy for any single step in transport. However, the value of E_a under conditions A–C should mainly reflect the activation energy for the reaction step $T_i \rightarrow T_o$. Similarly, the value of E_a under condition D should be close to that for the reaction step $S + T_i \rightarrow T_oS$. Clearly, the activation energy for the conformational change of the unoccupied transporter (conditions A–C) is significantly greater than that of the occupied transporter (condition D).

Comparison of Parameter Values with Literature Ones. While this study was in progress, Lowe and Walmsley (1986) determined the value of V_{max} and K_m for glucose transport in human erythrocytes at several temperatures under conditions of zero trans influx, zero trans efflux, and equilibrium exchange. In terms of Scheme I, each of the constants from these steady-state measurements (V_{max} and K_m from zero trans influx, zero trans efflux, and equilibrium exchange) is a complex constant, consisting of two or more of the individual constants in Scheme I. However, from the fact that the value V_{max} for equilibrium exchange is much larger than the values of V_{max} for zero trans uptake and exit at 0 °C, it is possible to deduce the individual values of k_{-1} and k_1. Moreover, the Arrhenius plots for V_{max} for zero trans efflux and equilibrium exchange are curved. Lowe and Walmsley made the assumption that this curvature arises as a result of the different activation

Table IV: Comparison of Constants Obtained from Single Half-Turnover and Steady-State Kinetics

constant	single half-turnover[a]	steady state[b]
k_1 (s^{-1})	9	87
k_{-1} (s^{-1})	5.2	10.8
k_2/K_{So} (mM^{-1} s^{-1})	66	190
k_{-2}/K_{Si} (mM^{-1} s^{-1})	31	23
E_a for k_{-1} (kcal/mol)	28.2[c]	41
E_a for k_{-2}/K_{si} (kcal/mol)	17.4[d]	18

[a] Values in this study at 10 °C. [b] Values from Lowe and Walmsley (1986) at 10 °C. [c] Value from condition C in Figure 4. [d] Value from condition D in Figure 4.

energies for the individual constants contributing to these composite constants. Through the use of this assumption, it was then possible to calculate the values of all the individual constants in Scheme I.

Our values and those of Lowe and Walmsley at 10 °C are presented in Table IV. With the exception of the values for k_1, which differ by a factor of 10, the values for the other rate constants agree within a factor of 3. Moreover, our values and theirs of the activation energies for k_{-1} and k_{-2}/K_{Si} are similar. When one considers that results from the steady-state measurements are for the intact erythrocyte, with its asymmetric distribution of membrane lipids (op den Kamp, 1979), whereas our results are for the purified transporter reconstituted in unsealed membranes of erythrocyte lipids, this agreement is very good. It shows that the purified, reconstituted transporter functions very similarly to the transporter in the erythrocyte.

References

Angyal, S. J. (1968) *Aust. J. Chem. 21*, 2737–2746.

Appleman, J. R., & Lienhard, G. E. (1985) *J. Biol. Chem. 260*, 4575–4578.

Baker, G. F., Basketter, D. A., & Widdas, W. F. (1978) *J. Physiol. 278*, 377–388.

Baldwin, J. M., Lienhard, G. E., & Baldwin, S. A. (1980) *Biochim. Biophys. Acta 599*, 699–714.

Baldwin, S. A., & Lienhard, G. E. (1981) *Trends Biochem. Sci. 6*, 208–211.

Baldwin, S. A., Baldwin, J. M., & Lienhard, G. E. (1982) *Biochemistry 21*, 3836–3842.

Barnett, J. E. G., Holman, G. D., Chalkley, R. A., & Munday, K. A. (1975) *Biochem. J. 145*, 417–429.

Carruthers, A. (1988) *Trends Biochem. Sci. 13*, 426–427.

Carruthers, A., & Melchior, D. L. (1985) *Biochemistry 24*, 4244–4250.

Christian, S. D., & Tucker, E. E. (1972) *Am. Lab. (Fairfield, Conn.) 14*, 31–36.

Deves, R., & Krupa, R. M. (1978) *Biochim. Biophys. Acta 510*, 186–200.

Gorga, F. R., & Lienhard, G. E. (1981) *Biochemistry 20*, 5108–5113.

Gorga, F. R., & Lienhard, G. E. (1982) *Biochemistry 21*, 1905–1908.

Lowe, A. G., & Walmsley, A. R. (1986) *Biochim. Biophys. Acta 857*, 146–154.

Mueckler, M., Caruso, C., Baldwin, S. A., Panico, M., Blench, I., Morris, H. R., Allard, W. J., Lienhard, G. E., & Lodish, H. F. (1985) *Science 229*, 941–945.

Naftalin, R. J. (1988) *Trends Biochem. Sci. 13*, 425–426.

Op den Kamp, J. A. F. (1979) *Annu. Rev. Biochem. 48*, 47–71.

Walmsley, A. R. (1988) *Trends Biochem. Sci. 13*, 226–231.

Turkey Gizzard Caldesmon: Molecular Weight Determination and Calmodulin Binding Studies†

Dean A. Malencik, Juan Ausio, Christine E. Byles, Brett Modrell, and Sonia R. Anderson*

Department of Biochemistry and Biophysics, Oregon State University, Corvallis, Oregon 97331-6503

Received May 19, 1989

ABSTRACT: Sedimentation equilibrium and sedimentation velocity measurements demonstrate that turkey gizzard caldesmon is an elongated molecule of molecular mass 75 ± 2 kDa. The frictional ratio (2.14) is consistent with a prolate ellipsoid of axial ratio 24, corresponding to an apparent length and width of 516 and 21.5 Å, respectively. As was previously determined for chicken gizzard caldesmon [Graceffa, P., Wang, C.-L. A., & Stafford, W. F. (1988) *J. Biol. Chem. 263*, 14196–14202], this molecular weight is appreciably smaller than the value (~135 000) estimated from the results of $NaDodSO_4$ gel electrophoresis experiments. However, a significant difference between the true molecular weights of turkey and chicken gizzard caldesmons—75 000 versus 93 000—also points to probable molecular weight variations within the subclass. Binding measurements, based on perturbation of the intrinsic tryptophan fluorescence of caldesmon in the presence of calmodulin, show that the interaction between the two proteins is strongly ionic strength and temperature dependent. Dissociation constants of 0.075 and 0.38 μM were determined in solutions containing 0.1 and 0.2 M KCl, respectively, at 24.3 °C. Fluorescence emission spectra and fluorescence anisotropy excitation spectra indicate that the tryptophanyl residues of caldesmon are located in solvent-accessible regions of the molecule, where they exhibit a high degree of mobility even when calmodulin is bound.

The caldesmons, major calmodulin and actin binding proteins in smooth muscle and nonmuscle cells, comprise two classes of immunoreactive polypeptides having apparent molecular weights of 120 000–150 000 and 71 000–77 000 (Bretscher & Lynch, 1985). Caldesmon was originally identified in chicken gizzard as the 120–150-kDa species and shortly thereafter found to inhibit the actin-activated adenosinetriphosphatase activity of phosphorylated myosin (Sobue et al., 1981, 1982).

† This research was supported by grants from the National Institutes of Health (DK13912) and the Muscular Dystrophy Association.

* Address correspondence to this author.

0006-2960/89/0428-8227$01.50/0